nature neuroscience

ARTICLES

Asymmetrical β-actin mRNA translation in growth cones mediates attractive turning to netrin-1

Kin-Mei Leung[1,3], Francisca PG van Horck[1,3], Andrew C Lin[1], Rachel Allison[2], Nancy Standart[2] & Christine E Holt[1]

Local protein synthesis regulates the turning of growth cones to guidance cues, yet little is known about which proteins are synthesized or how they contribute to directional steering. Here we show that β-actin mRNA resides in *Xenopus laevis* retinal growth cones where it binds to the RNA-binding protein Vg1RBP. Netrin-1 induces the movement of Vg1RBP granules into filopodia, suggesting that it may direct the localization and translation of mRNAs in growth cones. Indeed, a gradient of netrin-1 activates a translation initiation regulator, eIF-4E-binding protein 1 (4EBP), asymmetrically and triggers a polarized increase in β-actin translation on the near side of the growth cone before growth cone turning. Inhibition of β-actin translation abolishes both the asymmetric rise in β-actin and attractive, but not repulsive, turning. Our data suggest that newly synthesized β-actin, concentrated near sites of signal reception, provides the directional bias for polymerizing actin in the direction of an attractive stimulus.

Axonal growth cones navigate through the developing nervous system in response to guidance cues. To turn appropriately in response to guidance cue gradients, they transduce extracellular gradients into intracellular asymmetry. Previous studies have shown that guidance cue gradients induce asymmetries of signaling components such as calcium (Ca^{2+}; ref. 1) and receptor association with lipid rafts[2]. Similarly, turning can be induced by artificial asymmetries of Ca^{2+} (refs. 3,4), lipid rafts[2], phospholipase Cγ activation[5] or cyclic AMP (cAMP)[6]. Previous findings showed that chemotropic responses to netrin-1, semaphorin 3A (Sema3A), Slit2 and brain-derived neurotrophic factor (BDNF) require local translation[7–10], raising the question of whether asymmetrical protein synthesis influences growth cone turning in guidance cue gradients.

β-actin is a candidate for asymmetrical cue-induced synthesis. Of the three isoforms of actin, α, β and γ, β-actin is the isoform implicated in directional movement[11]. *In situ* hybridization shows that β-actin mRNA is present in axonal growth cones[9,12], and stimulation with neurotrophins, such as neurotrophin 3 (NT-3), BDNF or nerve growth factor, increases the transport of β-actin mRNA in both embryonic and adult axons[13–15]. Asymmetric actin polymerization is thought to be important in growth cone turning, as asymmetrical application of cytochalasin, an actin depolymerizing drug, causes repulsive turning[16]. These findings suggest that asymmetrical β-actin synthesis may be involved in growth cone turning.

Protein synthesis is regulated by translation initiation factors that globally regulate the recruitment of ribosomes to mRNAs[17]. Guidance cues such as netrin-1 and Sema3A activate the rate-limiting translation initiation factor eIF4E[10]. mRNA-specific regulation can be achieved by RNA-binding proteins that bind to target mRNAs, transport them to a specific cytoplasmic compartment and, in some cases, help regulate or silence their translation[18]. The localization of β-actin mRNA requires a *cis*-acting element located in the 3′ untranslated region (UTR) of the mRNA, called the 'zipcode'[19]. In chick, zipcode binding protein 1 (ZBP1) associates with the zipcode to regulate the localization of β-actin mRNA to the leading edge of fibroblasts and growth cones[14,19], and evidence showed that β-actin translation can be regulated by the phosphorylation of ZBP1 through Src kinase[20]. The *X. laevis* homolog of ZBP1, Vg1RBP (also known as Vera), is required for the motility of neural crest cells, binds several mRNAs such as those encoding Vg1, VegT and cofilin, and controls mRNA localization in *X. laevis* oocytes[8,21]. However, it is not known whether it binds to β-actin mRNA or whether it is present in developing retinal axons where it might help to regulate translation-dependent steering.

Here we investigate the mechanisms that underlie protein synthesis–dependent steering of growth cones to netrin-1. We show that netrin-1 stimulates a rapid translocation of Vg1RBP granules into filopodia and increases β-actin synthesis. A directional gradient of netrin-1 induces a translation-dependent increase in β-actin on the side of the growth cone closest to the gradient source (near side) and a similarly asymmetric activation of a global translational regulator (4EBP). These asymmetric changes precede growth cone turning, and inhibition of β-actin synthesis by antisense morpholinos blocks the netrin-1–induced attractive turning, suggesting that spatially asymmetric translation of β-actin, biased to the near side, directs turning toward the stimulus.

[1]Departments of Physiology, Development and Neuroscience and [2]Biochemistry, University of Cambridge, Downing Street, Cambridge CB2 3DY, UK. [3]These authors contributed equally to this work. Correspondence should be addressed to C.E.H. (ceh@mole.bio.cam.ac.uk).

Received 17 July; accepted 28 August; published online 17 September 2006; doi:10.1038/nn1775

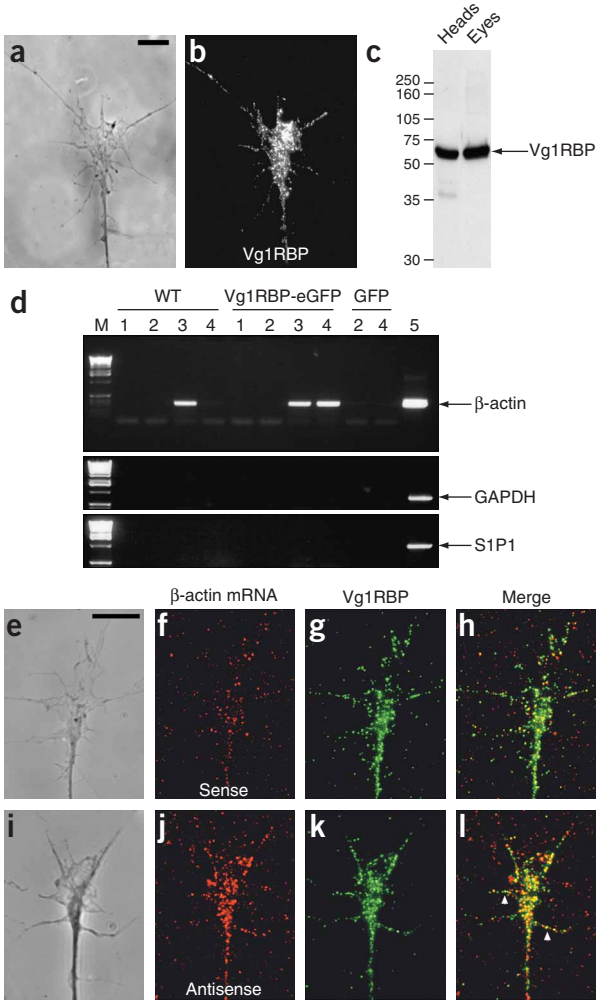

Figure 1 Vg1RBP is expressed in retinal growth cones and interacts with β-actin mRNA. (**a**,**b**) Cultured stage 33/34 retinal explants were stained with Vg1RBP antibody (**a**, phase; **b**, antibody to Vg1RBP). Vg1RBP is detected in the axon shaft, central domain and filopodia. (**c**) Western blot analysis using Vg1RBP antibody shows a predominant 65-kDa band in stage 33/34 head or eye lysates. (**d**) Vg1RBP was immunoprecipitated from head lysates of stage 33/34 wild-type (WT) embryos, injected with Vg1RBP-eGFP mRNA or GFP mRNA. RNA extracted from the immunoprecipitates was subjected to RT-PCR using primers to the 3′ UTR of β-actin mRNA (top), GAPDH mRNA (middle) or S1P1 mRNA (bottom). Lane 1, protein A beads only; lane 2, purified rabbit IgG; lane 3, Vg1RBP antiserum; lane 4, GFP antiserum; lane 5, positive RT-PCR control; lane M, molecular DNA marker. The β-actin mRNA is immunoprecipitated with both Vg1RBP and Vg1RBP-eGFP. GAPDH and S1P1 mRNAs do not interact with Vg1RBP. (**e**–**l**) FISH using riboprobes directed against the 3′ UTR of β-actin mRNA (**j**, antisense) or control RNA (**f**, sense) together with immunostaining of Vg1RBP (**g**,**k**) reveals partial colocalization of Vg1RBP and β-actin mRNA in the growth cone (**e**,**i**, phase; **f**, control sense RNA; **j**, β-actin antisense RNA; **g**,**k**, Vg1RBP; **h**,**l**, merge). Arrowheads refer to complexes of Vg1RBP and β-actin mRNA in a filopodium. Scale bars, 5 μm.

RESULTS

Vg1RBP interacts with β-actin mRNA in retinal growth cones

Immunostaining with an antibody to *X. laevis* Vg1RBP showed abundant expression of Vg1RBP in retinal growth cones in culture between stages 24 and 40 (**Fig. 1a**,**b**). Consistent with RNA-binding protein assembly in granules[22], Vg1RBP protein has a punctate distribution along the axon shaft and in the growth cone central domain and filopodia (**Fig. 1b**). On western blot analysis, the Vg1RBP antibody detected a predominant band of the expected size (65 kDa) in both head and eye lysates, verifying the specificity of the antibody (**Fig. 1c**).

Vg1RBP associates with β-actin mRNA as shown by immunoprecipitation followed by reverse transcription-polymerase chain reaction (RT-PCR; **Fig. 1d**). β-actin mRNA was detected by RT-PCR in samples immunoprecipitated from embryo head lysates using antibodies to endogenous Vg1RBP or expressed Vg1RBP-eGFP (**Fig. 1d**, lanes 3 and 4), but not in control immunoprecipitates (**Fig. 1d**, lanes 1 and 2). In contrast, the GAPDH and S1P1 (encoding sphingosine-1-phosphate receptor 1) mRNAs, the latter of which is present in retinal growth cones (L. Strochlic and C.E.H., unpublished data), did not associate with Vg1RBP (**Fig. 1d**, middle and bottom).

Association of β-actin mRNA and Vg1RBP *in vitro* does not prove that Vg1RBP binds β-actin mRNA *in vivo*. To investigate whether Vg1RBP and β-actin mRNA interact in the growth cone, we performed fluorescence *in situ* hybridization (FISH) with digoxigenin-labeled antisense probes to the β-actin 3′ UTR followed by immunostaining for endogenous Vg1RBP (**Fig. 1e–l**). Consistent with previous studies[12,14], we found a punctate pattern of the β-actin mRNA signal in growth cones (**Fig. 1i–l**). In contrast, FISH using sense probes detected only background signal (**Fig. 1e–h**). Vg1RBP granules overlapped with β-actin mRNA puncta compared with sense riboprobe puncta (antisense versus sense: 56.7% ± 1.2% versus 38.5% ± 1.0%, mean ± s.e.m., $P < 0.0001$ Mann-Whitney test), indicating significant colocalization of Vg1RBP and β-actin mRNA. Vg1RBP/β-actin mRNA complexes were also detected in the growth cone filopodia (**Fig. 1l**, arrowheads). These data indicate that Vg1RBP interacts with β-actin mRNA and suggest that Vg1RBP may, like ZBP1, transport β-actin mRNA to and within retinal growth cones.

Dynamic movements of Vg1RBP–eGFP granules in growth cones

mRNA transport in neuronal cells involves both anterograde and retrograde movements of messenger ribonucleoprotein (mRNP) complexes[14]. mRNP complexes are actively transported along microtubules and actin filaments[23]. We therefore investigated whether Vg1RBP granules show characteristics of active transport (**Fig. 2**).

To this end, we visualized Vg1RBP dynamics using live cell imaging of single growth cones expressing eGFP-tagged Vg1RBP. Vg1RBP-eGFP mRNA was introduced by blastomere injection at the eight-cell stage and retinal cultures were made from eGFP-expressing embryos at stage 33/34. Both endogenous and eGFP-tagged proteins were recognized by the Vg1RBP antibody using immunostaining or western blot analysis and show similar granular localization patterns and levels of expression (**Fig. 2a–e**). Furthermore, both endogenous Vg1RBP and Vg1RBP-eGFP can interact with β-actin mRNA *in vitro* (**Fig. 1d**).

Live cell imaging revealed bidirectional movements of Vg1RBP-eGFP granules in retinal growth cones (**Fig. 2f–i** and **Supplementary Video 1** online). In unstimulated cultures, Vg1RBP-eGFP granules were enriched in the growth cone central domain and were also occasionally observed in filopodia. Granule movement patterns ranged from oscillations with no net movement, to unidirectional and bidirectional movements over short and longer (> 10 μm) distances. The average speed ranged from 0 to 0.7 μm s^{-1}. Interference with the actin cytoskeleton by cytochalasin D resulted in a complete retraction of Vg1RBP granules from the growth cone (**Supplementary Video 2**

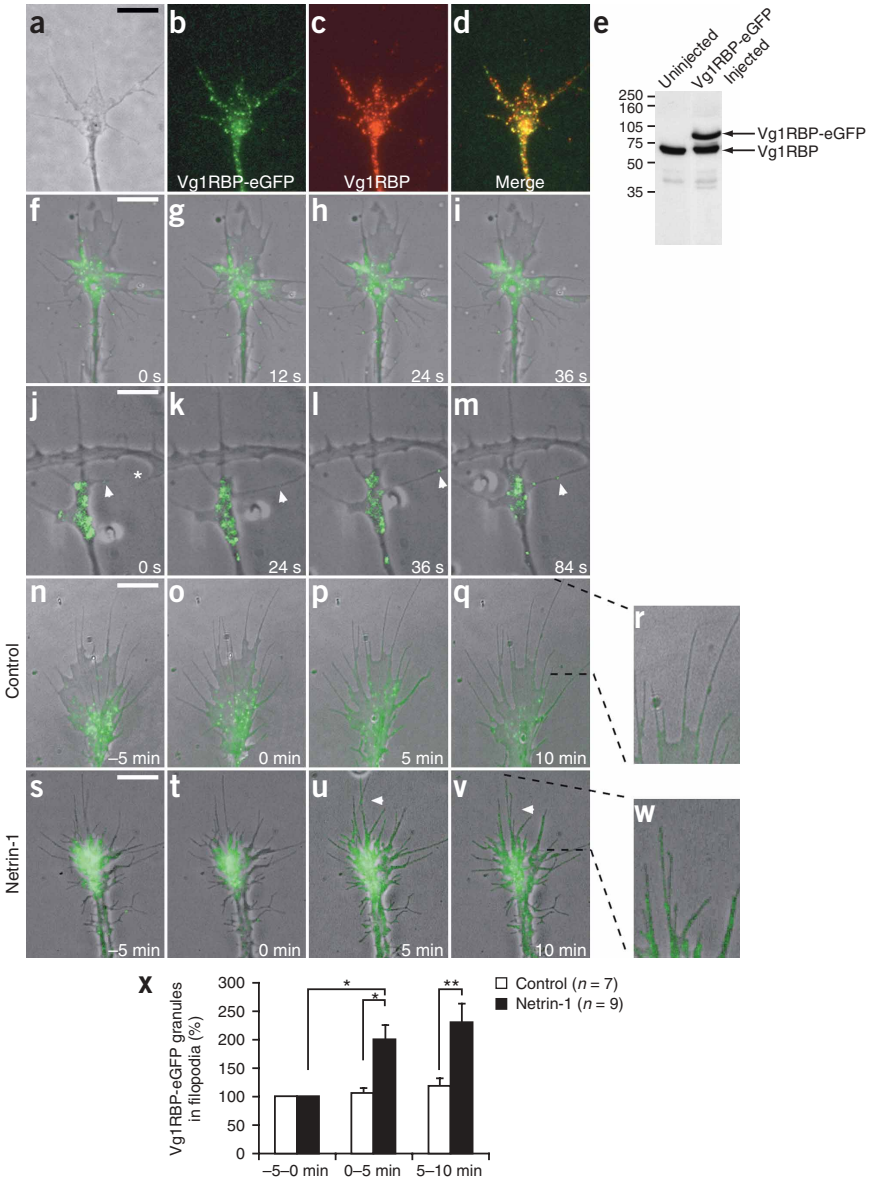

Figure 2 Netrin-1 or cell-contact induce translocation of Vg1RBP-eGFP into filopodia. (**a**–**d**) Retinal explants taken from stage 33/34 embryos expressing Vg1RBP-eGFP were stained with Vg1RBP antibody. Both endogenous and overexpressed proteins are recognized by the Vg1RBP antibody and show similar patterns of localization (**a**, phase; **b**, Vg1RBP-eGFP; **c**, Vg1RBP; **d**, merge). (**e**) Vg1RBP-eGFP is expressed at similar levels as the endogenous Vg1RBP, as shown by western blot analysis of head lysates from injected and uninjected embryos. (**f**–**m**) Time-lapse analysis of Vg1RBP-eGFP shows bidirectional movement of Vg1RBP-eGFP granules in the axon shaft, growth cone central domain and filopodia. Images were taken every 12 s (**f**–**i** and **Supplementary Video 1**). Vg1RBP-eGFP granules are also detected moving along filopodial contact-contact sites (**j**–**m**, arrowheads, and **Supplementary Video 2**). The asterisk indicates the branch/filopodium, which is going to contact the filopodium expressing Vg1RBP-eGFP. (**n**–**w**) Live imaging of Vg1RBP-eGFP expressing retinal growth cones stimulated with control medium (**n**–**r**) or netrin-1 (**s**–**w** and **Supplementary Video 3**) at $T = 0$ min. (**x**) The percentage of Vg1RBP-eGFP granules in the filopodia was calculated in each frame and averaged per 5 min. Application of netrin-1 results in an increase of Vg1RBP-eGFP granules in the filopodia compared with control. $^{*}P < 0.05$, $^{**}P < 0.01$, Kruskal-Wallis test. Error bars are s.e.m. Scale bars, 5 μm.

online). In contrast, depolymerizing microtubules with nocodazole had no obvious effects on Vg1RBP movement in the growth cone (data not shown).

Filopodia can be considered as the long-range (5- to 10-μm) sensors of the growth cone, enabling it to detect and respond to new cues along the pathway. It is interesting, therefore, that we occasionally observed Vg1RBP granules moving rapidly to the site where a filopodium forms a new contact with another filopodium or axon shaft (**Fig. 2j–m**). An example is shown (**Fig. 2j–m** and **Supplementary Video 3** online) of anterograde transport of a Vg1RBP-eGFP granule moving to, and subsequently away from, a transient contact site between two filopodia (different cellular origins). This suggests that the trafficking of Vg1RBP granules in filopodia might be regulated by external cues.

Netrin-1 induces transport of Vg1RBP into filopodia

The observation that Vg1RBP granules move to contact sites prompted us to investigate whether an axon guidance cue could alter granule movement. Netrin-1 has an important role in retinal axon guidance[24] and can trigger local protein synthesis in growth cones[10]; therefore, we hypothesized that it might also elicit the transport of Vg1RBP granules into filopodia to bring mRNA close to sites of signal reception. To test this, we used live imaging to determine the percentage of Vg1RBP-eGFP granules in the central domain versus filopodia before and during global stimulation with netrin-1 (**Fig. 2n–x**). Bath application of netrin-1, but not control medium, increased the percentage of Vg1RBP granules present in filopodia after 5 and 10 min (**Supplementary Video 4** online). The percentage of granules in the central domain of the growth cone did not change significantly (data not shown) and no obvious changes in growth cone morphology were observed. Netrin-1 also increased diffuse Vg1RBP signal in filopodia, which was not included in the quantification (**Fig. 2x**). To test whether these Vg1RBP granules contain β-actin mRNA, we used quantitative immunofluorescence (QIF)/FISH. Netrin-1 induced an increase in both Vg1RBP and β-actin mRNA signal in filopodia after 10 min. Moreover, similar levels of colocalization between Vg1RBP and β-actin mRNA in filopodia were detected before and after netrin-1 stimulation (**Supplementary Fig. 1** online). These results show that netrin-1 induces the transport of Vg1RBP granules into the filopodia and suggest that a substantial fraction of these carry β-actin mRNA cargo.

Netrin-1 triggers a translation-dependent rise in β-actin

As netrin-1 regulates the movement of an RNA-binding protein that can interact with β-actin mRNA, we examined whether netrin-1 might trigger β-actin mRNA translation in growth cones (**Fig. 3**). QIF using an antibody to β-actin revealed a 30% increase in the average pixel intensity per unit area after 5-min stimulation with netrin-1

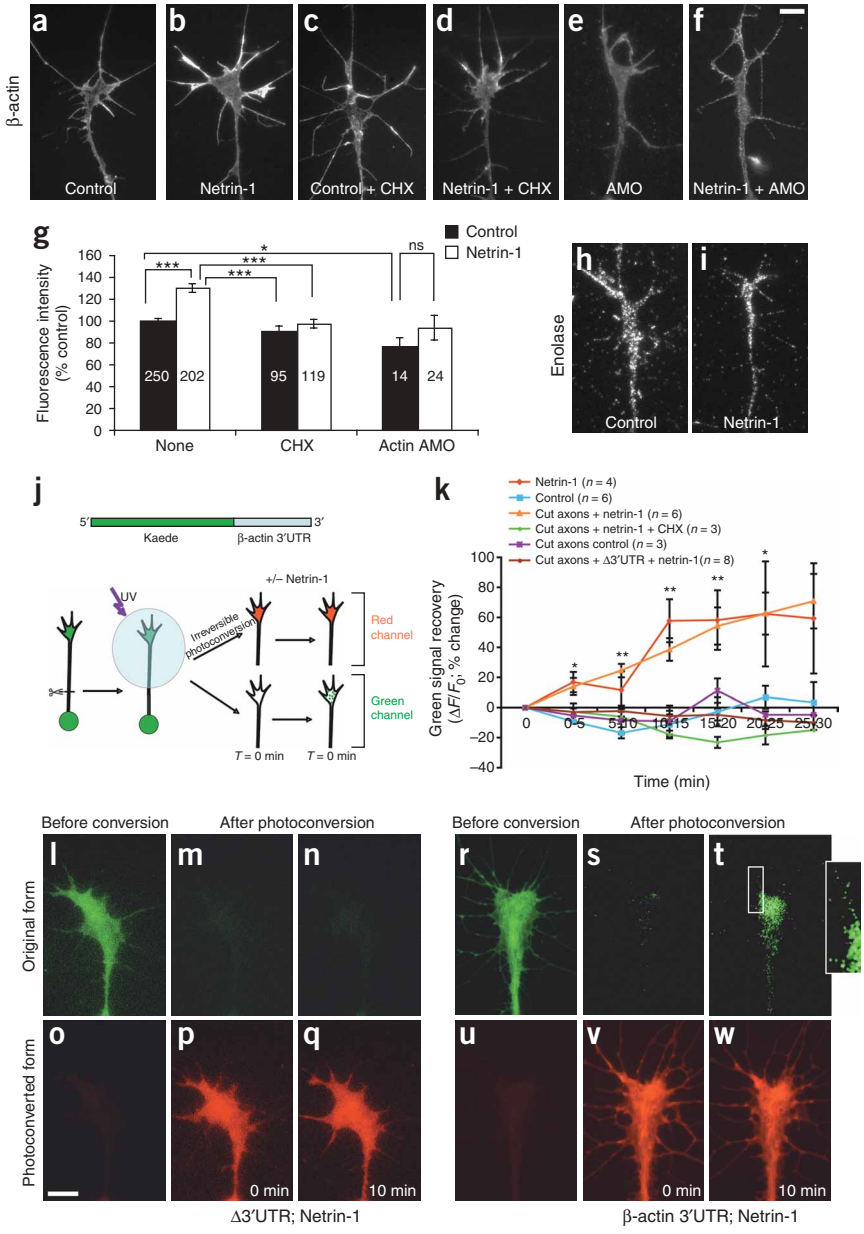

Figure 3 Netrin-1 induces β-actin translation driven by its 3′ UTR. (**a**–**g**) Stage 24 retinal growth cones were stimulated with netrin-1 for 5 min, stained for β-actin and fluorescence intensities measured. Netrin-1 induced an increase in β-actin QIF signal, which was blocked by CHX and β-actin AMO. $^{***}P < 0.0001$, Kruskal-Wallis test. Growth cones from β-actin AMO–injected retina showed reduced β-actin QIF signal (**e**,**g**), which was not affected by netrin-1 stimulation (**f**,**g**). $^{*}P = 0.02$, Mann-Whitney test. NS, non-significant. (**h**,**i**) Enolase QIF signal was not affected by netrin-1 stimulation. (**j**) Schematic diagram of Kaede construct and experimental design. (**l**–**w**) Time-lapse imaging showed that only Kaede-green was detected before photoconversion (**l**,**r**). At $T = 0$ min, Kaede was photoconverted and only Kaede-red was detected (**p**,**v**). Netrin-1 had no effect on Kaede-green (**l**–**n**) or Kaede-red signals (**o**–**q**) in growth cones expressing Kaede-3′ UTR (**k**). However, netrin-1 induced a recovery of Kaede-green in both intact and severed growth cones expressing Kaede-β actin 3′ UTR (**k**,**s**,**t**), which was blocked by CHX (**k**). The recovery was also seen in some filopodia (**t**, boxed area and inset). The exposure gain for the inset was increased for visualization of filopodia. Kaede-red remained unchanged (**v**,**w**). The change in Kaede-green signal (ΔF) was compared with the image taken at $T = 0$ min (F_0) and presented as $\Delta F / F_0$. $^{*}P < 0.05$, $^{**}P < 0.01$, Mann-Whitney test. Scale bars, 5 μm. Error bars are s.e.m. Numbers inside the bars indicate the number of growth cones analyzed.

(**Fig. 3a**,**b**,**g**) compared with unstimulated growth cones[8,10,25]. Cycloheximide (CHX), a protein synthesis inhibitor, blocked this increase (**Fig. 3c**,**d**,**g**) but did not significantly affect growth cone β-actin mRNA abundance (control versus CHX: 100% ± 6.2% versus 93% ± 6.8%, mean ± s.e.m., $P = 0.106$ Mann-Whitney test), suggesting that the netrin-1–induced increase in β-actin protein is mediated through protein synthesis. A blocking antibody to deleted in colorectal cancer (DCC), the receptor that mediates growth cone chemotropic responses to netrin-1 (ref. 24), also prevented this increase in β-actin QIF signal, indicating that the effects of netrin-1 on translation are mediated by DCC (**Supplementary Fig. 2** online).

To specifically inhibit β-actin translation, we used an antisense morpholino oligonucleotide (AMO) directed against the AUG start site of β-actin mRNA. Lissamine-tagged AMOs were injected into blastomeres fated to give rise to eyes. At the concentrations used, the AMO-injected embryos developed normally and retinal cultures were made from lissamine-positive eyes at stage 24. Fluorescence labeling of AMOs enabled us to restrict our analyses to growth cones known to contain AMOs (**Supplementary Fig. 2** online). The β-actin QIF signal was significantly lower in AMO-containing growth cones than in control growth cones (23%; $P = 0.02$, Mann-Whitney test; **Fig. 3a**,**e**,**g**), verifying that the β-actin AMO inhibits β-actin translation. Moreover, netrin-1 did not significantly alter β-actin QIF signal in AMO-containing growth cones $P = 0.10$, Mann-Whitney test; indicating that the netrin-1–induced rise in β-actin abundance depends on translation of β-actin mRNA (**Fig. 3f**,**g**).

In contrast, the QIF signal of a noncytoskeletal protein, enolase, whose mRNA is abundant in retinal growth cones (L. Strochlic and C.E.H., unpublished data), remained unchanged after netrin-1 stimulation (**Fig. 3h**,**i**; control versus netrin-1: 100% ± 5% versus 97% ± 4%, mean ± s.e.m., $P = 0.648$ unpaired t-test), indicating that netrin-1 does not elicit the translation of all mRNAs present in growth cones. Consistent with this, a previous study in *X. laevis* retinal growth cones showed that netrin-1 does not induce translation of cofilin mRNA, whereas Slit2, a repellent guidance factor, induces the translation of cofilin but not β-actin mRNA[8]. To test whether β-actin translation is a common response to attractants, we used a second chemoattractant, BDNF, that has been shown to increase protein synthesis in neurons[27] and elicits protein synthesis–dependent turning responses in *X. laevis* spinal neurons[7]. We found that exposure of retinal growth cones to BDNF increased the β-actin QIF signal by 61% in 10 min and that this rise was blocked by CHX (**Supplementary Fig. 2** online). These results suggest that β-actin mRNA is translated locally in growth cones in response to chemoattractants.

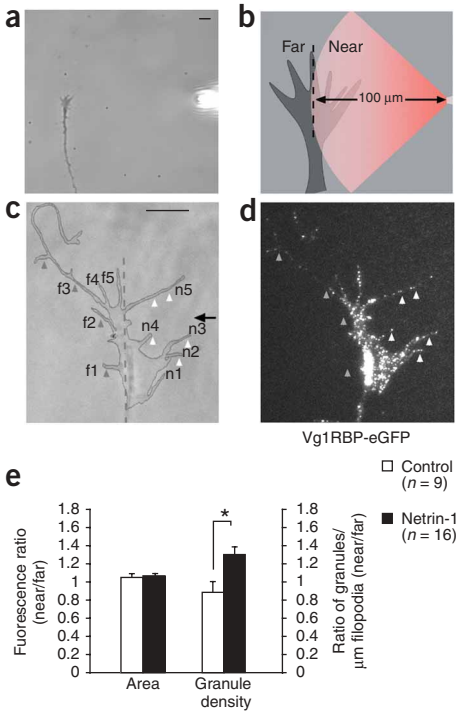

Figure 4 Vg1RBP granules move into filopodia closest to a netrin-1 source. (**a**,**b**) The experimental design shows the pipette tip positioned 100 μm from the growth cone at an angle of 90°; a dashed line divides the growth cone into near and far sides with respect to the pipette. (**c**–**e**) Vg1RBP-eGFP–expressing retinal growth cones were stimulated with a gradient of culture medium (control) or netrin-1 for 5 min and subsequently fixed. Mean fluorescence intensities as well as the number of granules per μm filopodia were calculated for both the near and far sides. A gradient of netrin-1 induces an increase in the number of Vg1RBP-eGFP granules per μm filopodia at the near side. No difference in Vg1RBP fluorescence intensity was observed in the far versus the near side (**e**). Near-side and far-side filopodia are numbered n1–n5 and f1–f5, respectively. Arrowheads indicate filopodia containing low-density (gray arrowheads) and high-density (white arrowheads) areas of Vg1RBP-eGFP granules. $^*P < 0.03$ Mann-Whitney test. Arrow indicates the direction of the pipette. Error bars are s.e.m. Scale bars, 5 μm.

β-actin 3′ UTR mediates netrin-1–induced reporter synthesis

The translation of mRNAs is commonly regulated by the UTRs[28]. To test directly whether the β-actin 3′ UTR drives the synthesis of new protein in response to netrin-1, we constructed a photoconvertible fluorescent protein[29] linked to the β-actin 3′ UTR (Kaede–β-actin 3′ UTR; **Fig. 3j**). Kaede protein is originally green but can be irreversibly, proteolytically converted to the red form by ultraviolet illumination, thereby permitting the detection of newly synthesized protein by visualizing the return of green fluorescence. Plasmid cDNA encoding Kaede–β-actin 3′ UTR was introduced by blastomere injection and stage 24 eyes were cultured. Kaede-positive growth cones were illuminated by ultraviolet light for 6 s, which efficiently converted the green into red fluorescence (**Fig. 3j**,**l**–**q**). Netrin-1 stimulation significantly increased the green, but not red, signal within 5 min (**Fig. 3k**,**r**–**w**). This increase occurred mainly in the body of the growth cone but, with time, could also be detected in filopodia (**Fig. 3t**, inset). The elevation in Kaede-green occurred even when axons were severed from their cell bodies, demonstrating that the increase was not from new protein transported from the soma (**Fig. 3k**). Green fluorescence did not increase if the β-actin 3′ UTR was replaced by a control UTR mutated to escape regulation by Vg1RBP (Δ3′ UTR; **Fig. 3k**–**q**) or if growth cones received a control vehicle instead of netrin-1 (**Fig. 3k**). In fact, in these control conditions, there was a slight decrease in green fluorescence due to photobleaching, suggesting that the netrin-1–induced increase in green fluorescence is underestimated. The netrin-1–induced return of green fluorescence was blocked by CHX added before photoconversion (**Fig. 3k**), indicating that it represented the synthesis of new protein, not just folding of Kaede protein synthesized immediately before photoconversion. These data indicate that the β-actin 3′ UTR drives the translation of new protein in response to netrin-1.

Netrin-1 gradient induces asymmetric Vg1RBP transport

Our results with globally added netrin-1 suggest that guidance cues activate mechanisms that transport mRNA granules closer to sites of signal reception, potentially helping the growth cone respond to a directional stimulus. Thus, we reasoned that a directional stimulus might produce polarized transport of granules. To test this, we applied a netrin-1 gradient to growth cones and determined whether it elicited asymmetric trafficking of Vg1RBP. The gradient was produced by pulsatile ejection from a micropipette[6] positioned at a 90° angle to the growth cone (**Fig. 4a**,**b**) to achieve a steep difference between the 'near' and 'far' sides of the growth cone. The line of symmetry was determined by tracing the perpendicular from the pipette to the axon shaft. Retinal growth cones expressing Vg1RBP-eGFP were subjected to a gradient of netrin-1 or control medium for 5 min and then fixed and imaged. The number of granules per micrometer filopodia, as well as the average pixel intensity per unit area, was compared between the near and far sides of the growth cone, yielding a near/far ratio (**Fig. 4b**). Netrin-1, but not control medium, increased the number of granules per micrometer in filopodia on the near side by approximately 30% (**Fig. 4c**–**e**). Prolonged netrin-1 stimulation has been shown to increase filopodial length in retinal growth cones[30]. However, a 5-min directional stimulation with netrin-1 did not significantly change the average length of the filopodia at the far versus the near side (6.48 μm versus 6.22 μm; $P = 0.6$, paired t-test). Furthermore, the overall fluorescence intensity of each side did not change, indicating that the asymmetric distribution is due to local transport of granules (**Fig. 4e**). Thus, a netrin-1 gradient elicits the polarized transport of Vg1RBP into filopodia.

Netrin-1 gradient induces asymmetric 4EBP phosphorylation

Bath application of netrin-1 has been shown to cause the rapid phosphorylation of the translation initiation factor 4EBP[10]. The phosphorylation of 4EBP is a marker for cap-dependent translation initiation, because hypophosphorylated 4EBP blocks translation initiation by sequestering the rate-limiting translation initiation factor eIF-4E[17].We therefore examined whether a gradient of netrin-1 could similarly induce asymmetric 4EBP phosphorylation.

Growth cones were stimulated with a netrin-1 gradient for 5 min, fixed and double-stained for Ser65-phosphorylated-4EBP and total-4EBP (**Fig. 5a**). 4EBP is phosphorylated hierarchically, with Ser65 being the final residue phosphorylated[31]. We used two methods to assess asymmetric phosphorylation. First, the degree of phosphorylation on the near and far sides was taken as the ratio of phospho-4EBP to total-4EBP intensity per unit area (**Fig. 5b**). Phosphorylation asymmetry was calculated as the near/far ratio of 4EBP phosphorylation. Second, phosphorylation asymmetry was calculated as the difference between the 'centers of mass' of phospho-4EBP and total-4EBP intensity (**Fig. 5c**). By both methods, the netrin-1 gradient produced a significant asymmetry in 4EBP phosphorylation, whereas a control gradient did not (**Fig. 5d**–**h**).

4EBP is phosphorylated by the kinase target of rapamycin (TOR)[17]. To test whether asymmetrical phosphorylation of 4EBP is mediated by TOR, we used the inhibitor of TOR, rapamycin. Rapamycin-treated growth cones did not show any significant asymmetry in 4EBP phosphorylation (**Fig. 5d–h**). Although we cannot formally rule out the possibility that phospho-4EBP is selectively transported across the growth cone in a rapamycin-sensitive manner, the more parsimonious explanation is that an external gradient of netrin-1 is translated into an internal gradient of translation initiation through asymmetrical activation of signal transduction pathways.

Netrin-1 gradient elicits spatially asymmetric β-actin synthesis

As a netrin-1 gradient stimulates asymmetric activation of 4EBP and movement of Vg1RBP, we next determined whether it elicits changes dependent on asymmetric protein synthesis in β-actin. Growth cones were stimulated with a netrin-1 gradient for 5 min and immunostained for β-actin, and the near/far ratio of average pixel intensity per unit area was determined (**Fig. 6**). Growth cones stimulated with a netrin-1 gradient, but not control growth cones, commonly showed an asymmetric distribution of β-actin QIF signal with a near/far ratio of 1.35:1 (**Fig. 6a**,**b**,**f**). The netrin-1–induced near/far bias in β-actin QIF signal was abolished in growth cones treated with CHX or β-actin AMO (**Fig. 6c**,**d**,**f**). These observations show that a netrin-1 gradient induces an asymmetric rise in β-actin in growth cones that is abolished by inhibition of translation and specifically inhibition of β-actin mRNA translation, thereby implicating newly synthesized β-actin in establishing the asymmetry.

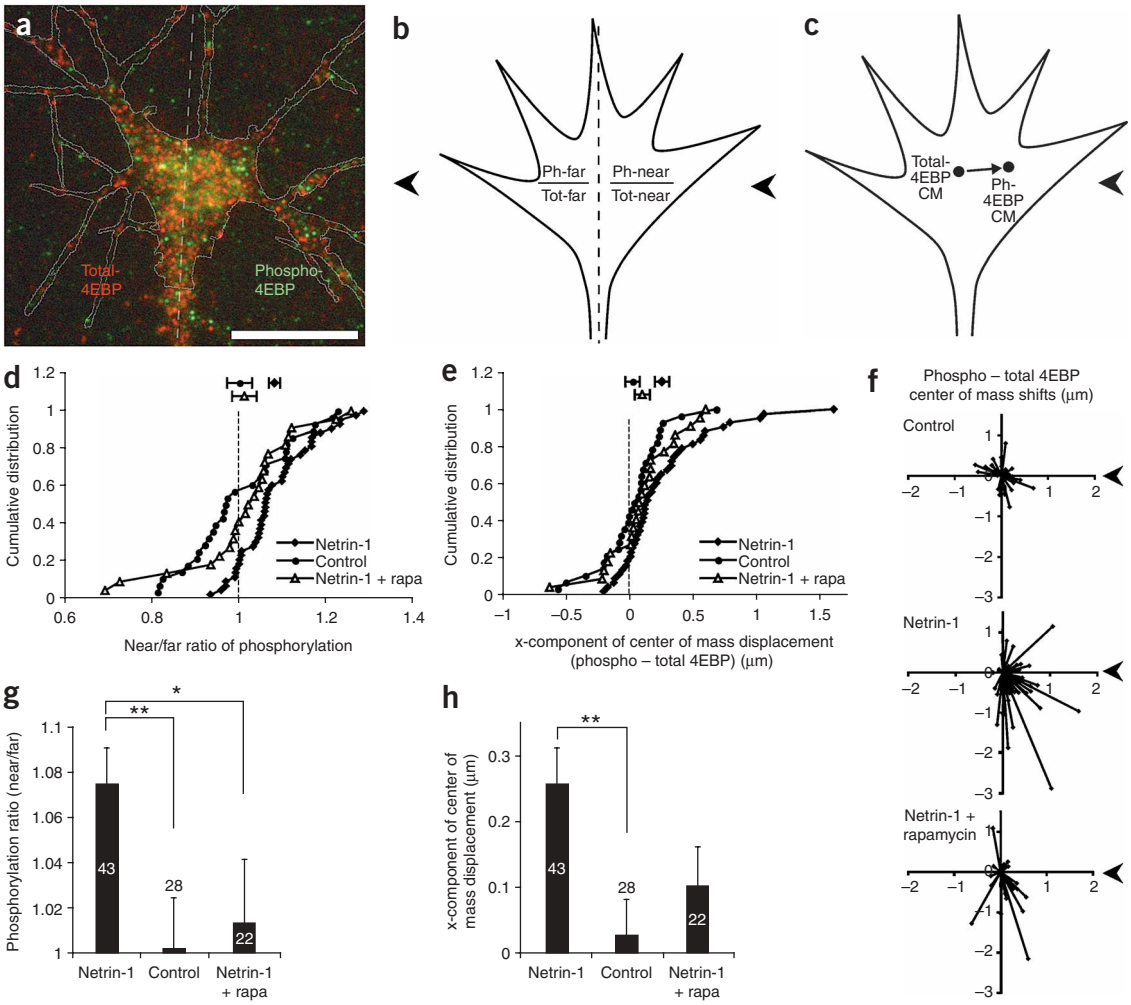

Figure 5 Netrin-1 gradient causes asymmetric activation of translation regulator. (**a**) A growth cone is shown double-stained for total-4EBP (red) and phospho-4EBP (green) with a line dividing the near and far sides. Lack of overlap may be due to stochastic mutual exclusion by large Zenon Fc-antibody complexes. (**b**,**c**) Asymmetric phosphorylation of 4EBP was assessed by the near/far ratio method (**b**) or by the center of mass method (**c**). (**d**–**h**) Phosphorylation is higher on the near side than on the far side in netrin-1–stimulated growth cones ($P < 0.000001$, paired *t*-test), but not in control-stimulated growth cones ($P = 0.9$) or netrin-1–stimulated growth cones treated with rapamycin (**d**,**g**; $P > 0.95$). The center of mass of phospho-4EBP staining is significantly closer to the pipette than that of total-4EBP in netrin-1–stimulated growth cones ($P < 0.0001$, paired *t*-test), but not in control-stimulated growth cones ($P > 0.65$) or netrin-1–stimulated growth cones treated with rapamycin (**e**,**h**; $P > 0.1$). The difference in center of mass shifts between the netrin-1 and netrin-1 + rapamycin conditions is almost significant ($P = 0.06$, Welch-corrected unpaired *t*-test). Vector plots of center of mass shifts show that only the netrin-1 condition shows consistent center of mass shifts toward the pipette (**f**). Each vector represents the center of mass shift of phospho-4EBP relative to total-4EBP in one growth cone. The axon shaft is down. Numbers in **g** and **h** indicate number of growth cones per condition. $^{**}P < 0.005$, $^{*}P < 0.05$, Welch-corrected unpaired *t*-test. Arrowheads indicate direction of pipette. Scale bar, 10 μm. Error bars are s.e.m.

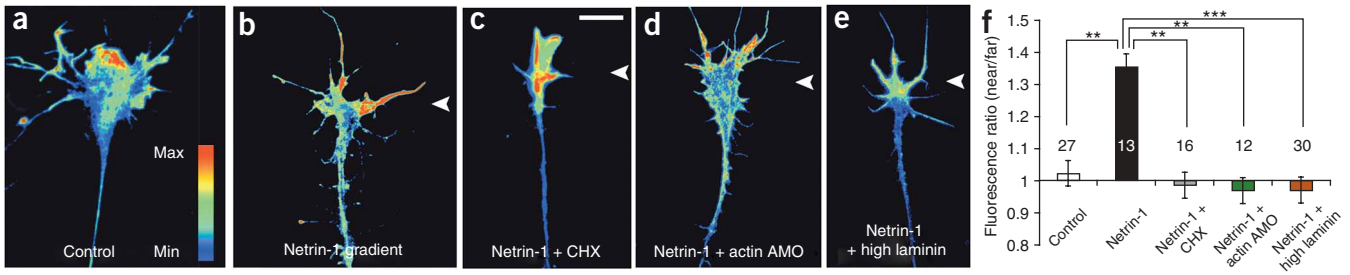

Figure 6 Netrin-1 gradient elicits asymmetric increase of β-actin across the growth cone. (**a**–**f**) Growth cones from stage 24 retinal explants were exposed to a gradient of netrin-1 for 5 min and then stained for β-actin. Fluorescence intensities of both sides of the growth cone were measured and the near/far ratios of the different groups were compared (**f**). In control conditions, β-actin was expressed at similar levels on both sides of the growth cone (**a**). Netrin-1 gradient induced an asymmetric rise in β-actin QIF signal on the near side (**b**), which was blocked by CHX (**c**) and β-actin AMO (**d**). Netrin-1 did not cause β-actin asymmetry in growth cones grown on high-laminin substrate (**e**). Images were pseudocolored (see color bar in **a**). $^{**}P = 0.003$, $^{***}P < 0.001$, Kruskal-Wallis test. Scale bar, 10 μm. Error bars are s.e.m. Numbers in **f** indicate the number of growth cones analyzed.

β-actin AMOs block netrin-1–induced attraction

Finally, we hypothesized that the spatially asymmetric translation of β-actin mRNA was critical to the turning response to netrin-1. To test this, β-actin synthesis was inhibited with β-actin AMOs during a standard turning assay with netrin-1 (ref. 30 and **Fig. 7**). Consistent with previous studies[30], growth cones were attracted by a netrin-1 gradient (**Fig. 7a–c,f**; mean turning angle 18.4°) but not by a control gradient (**Fig. 7c,f**; 0.9°). Growth cones containing control AMOs also turned toward the netrin-1 gradient (**Fig. 7c,f**; 13.1°), but growth cones containing β-actin AMOs were not attracted to a netrin-1 gradient (**Fig. 7c–f**; –0.7°). The absence of turning by the β-actin AMO growth cones was not due to compromised motility, because the average extension rate was not significantly different between β-actin AMO and control AMO growth cones (**Fig. 7e**; 0.28 μm min^{-1} versus 0.30 μm min^{-1}; $P = 0.7$, unpaired *t*-test), consistent with previous findings that protein synthesis is not required for axon extension[10,32]. These results suggest that the attractive turning to netrin-1 requires rapid, local β-actin synthesis.

To test whether AMOs inhibit the general responsiveness of growth cones to chemotropic cues, we examined whether β-actin AMO-containing growth cones were sensitive to repulsive cues. First, we used Sema3A and found that both the collapse and repulsive turning responses of β-actin AMO growth cones were indistinguishable from control growth cones, demonstrating that the sensitivity to repellents was not compromised (**Fig. 7j–l** and **Supplementary Fig. 2** online). Second, we used netrin-1 on growth cones grown on a high concentration of laminin (20 μg ml^{-1}), which converts attraction to repulsion by lowering cAMP levels in retinal growth cones[26,33]. Under these repulsive conditions, growth cones containing β-actin AMOs were also

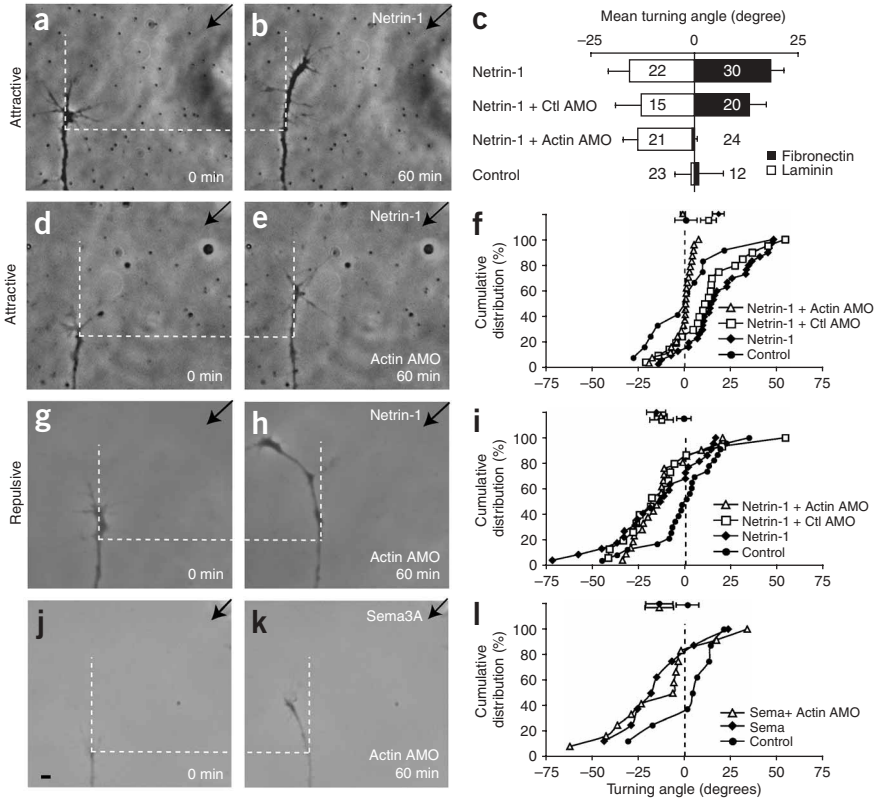

Figure 7 β-actin morpholinos block netrin-1–induced attractive turning. Eye primordia from stage 24 embryos injected with β-actin or control AMO were cultured for 24 h. (**a**–**i**) Under attractive conditions, netrin-1 caused strong positive turning (**a**–**c**,**f**; 18.4° ± 3.2°), whereas control medium did not (0.9° ± 6.0°). This attractive response was blocked in β-actin AMO-containing growth cones (**c**–**f**; –0.7° ± 1.3°), whereas growth cones containing control AMO retained attractive turning in response to netrin-1 (**c**,**f**; 13.1° ± 4.2°). $^{***}P < 0.001$. Under repulsive conditions, growth cones turned away from the source of netrin-1 (**c**,**i**, –15.8° ± 5.1°), but not control medium (–0.9° ± 3.9°). Introduction of β-actin AMO, as well as control AMO, into growth cones did not affect the repulsive turning response (**c**,**g**–**i**; –13.2° ± 3.3° and –12.8° ± 6.3°, respectively). $^{***}P < 0.001$. (**j**–**l**) The repulsive turning triggered by Sema3A in control growth cones (–13.6° ± 7.3°) is similar to that in β-actin AMO-containing growth cones (–13.6° ± 7.5°). $P > 0.05$. The control supernatant did not cause repulsive turning (1.5° ± 6.1°). The Kolmogorov-Smirnov test was used. Mean turning angle is shown ± s.e.m. Error bars are s.e.m. Scale bar, 5 μm.

repelled by a netrin-1 gradient (**Fig. 7c,g–i**; –13.2°). β-actin AMO and control AMO growth cones grew on laminin at the same rate (0.5 μm min^{-1}). Consistent with this, growth cones stimulated with a netrin-1 gradient for 5 min under these repulsive conditions did not show an asymmetric increase in β-actin QIF signal on the near side (**Fig. 6e,f**). A slight bias toward the far side was sometimes observed, but this was not statistically significant. Our results show that inhibition of β-actin translation differentially affects attractive and repulsive responses and that β-actin translation is of particular importance for attractive turning.

DISCUSSION

Our study addressed the question of whether asymmetrical protein synthesis has a role in growth cone turning. Our results indicate that new β-actin protein is synthesized in response to netrin-1 and that an external gradient of netrin-1 causes a polarized increase of β-actin on the side of the growth cone nearest to the source. The increase occurs just 5 min after addition of netrin-1 and is abolished by inhibitors of translation. Notably, β-actin AMOs block attractive, but not repulsive, turning suggesting that β-actin synthesis is particularly important for directional guidance toward a positive cue.

The finding that the β-actin AMOs abolished the netrin-1–induced increases in β-actin in growth cones indicates that the AMOs effectively inhibited β-actin translation over the time period examined (5–60 min). Overall, the AMOs caused a 20–25% drop in β-actin QIF signal. This relatively small knockdown of β-actin probably reflects the large maternal pool of actin that is recycled for the first 24–36 h of embryonic development and most likely predominates in the pioneering population of retinal axons, which develop just 28 h after fertilization. Indeed, the knockdown in β-actin QIF signal was higher in older growth cones than in younger ones (approximately 40% in stage 35/36 versus 23% in stage 24; data not shown). AMO-containing axons grew at a normal rate and showed appropriate chemotropic responses to Sema3A and netrin-1 under repulsive conditions. It could be argued that attractive turning is more sensitive to β-actin levels (and hence actin polymerization rates) than axon extension or repulsive turning, and that the β-actin AMO knocks down baseline β-actin translation levels just enough to block attractive turning, but not extension or repulsion. Such an argument, however, would predict that the AMO would at least reduce axon extension and repulsive turning, whereas in fact we observed that extension and repulsion remained normal. These lines of evidence indicate that β-actin translation is specifically required in attractive turning, but not in undirected growth, repulsive turning or general responsiveness to netrin-1.

What role does β-actin translation have in attractive turning? At first glance it would seem that β-actin synthesis is not necessary for actin polymerization given that the pool of unpolymerized actin in growth cones is thought to be large[34]. Indeed, it has been estimated that β-actin synthesis provides only 7% of the total actin needed for polymerization in migrating fibroblasts[19], making it unlikely that asymmetrical β-actin synthesis makes the growth cone turn by sheer mass alone. It has been proposed that newly synthesized β-actin can polymerize or nucleate polymerization more efficiently than 'older' actin as a result of chaperone binding to the nascent β-actin chain[11,35] and protecting it from glutathionylation, which restricts the rate of polymerization[36]. Thus, given that the rate-limiting step of actin polymerization is nucleation, an appealing model is that local β-actin synthesis provides spatially localized nucleation sites for actin polymerization[11,19,37]. The restricted size of the growth cone compartment would concentrate newly synthesized β-actin monomers in a small volume, thereby contributing to rapid formation of nucleation sites. We therefore suggest that a gradient of netrin-1 elicits spatially biased actin polymerization by inducing the asymmetric synthesis of β-actin and nucleation sites on the side of the growth cone closest to the pipette (**Supplementary Fig. 3** online). The netrin-1–stimulated increase in the β-actin signal is particularly evident in filopodia, suggesting that the new actin contributes to actin-filament bundles in these structures that radiate from the less-polarized actin mesh network in the body of the growth cone[38]. As β-actin synthesis occurs at least 10 min before overt turning, we hypothesize that asymmetrical β-actin translation prefigures the turn itself.

Asymmetrical synthesis requires spatial regulation of β-actin translation. One possible mechanism is transport of β-actin mRNA to the side closest to the source of the gradient. Previous studies have shown that the neurotrophin NT-3 elicits the transport of the β-actin mRNA-ZBP1 complex into growth cones[14] and serum stimulation induces the transport of β-actin mRNA to the leading edge of fibroblasts[39]. An independent study shows that both ZBP1 and β-actin mRNA become asymmetrically distributed in the growth cones of *X. laevis* spinal neurons upon BDNF stimulation[40]. In agreement with this study, our experiments show that Vg1RBP binds β-actin mRNA and that netrin-1 stimulation induces transport of Vg1RBP granules into filopodia, asymmetrically if netrin-1 is presented in a gradient. We also find that sites of filopodial contact can induce the transport of Vg1RBP-eGFP granules into filopodia, suggesting that external cues recruit RNA-binding proteins and their mRNA cargo to local sites of stimulation. Although our dynamic imaging studies could not demonstrate that the Vg1RBP-eGFP granules moving into filopodia were specifically transporting β-actin mRNA, fixed samples showed that Vg1RBP colocalizes with β-actin mRNA and the netrin-1–induced increase in filopodial Vg1RBP is accompanied by an increase in filopodial β-actin mRNA.

Another mechanism for spatial regulation of β-actin synthesis is the asymmetrical activation of translation. We found that a gradient of netrin-1 induced a significant asymmetry in the phosphorylation of the translation initiation factor 4EBP, suggesting a corresponding asymmetry in the global rate of translation. The translation of β-actin mRNA, like that of most eukaryotic mRNAs, is cap dependent[41], making it subject to asymmetrical activation of translation-initiation factors. Both attractants and repellents stimulate activation of translation initiation factors[10,42], although they presumably induce synthesis of different proteins. Indeed, in contrast to our result that netrin-1 stimulates synthesis of β-actin, the repellents Sema3A and Slit2 stimulate synthesis of RhoA and cofilin, respectively, which are proteins that promote actin depolymerization[8,9]. An external gradient can activate signaling cascades asymmetrically to generate an internal gradient of translation activation oriented toward both attractants and repellents, whereas the identity of the asymmetrically synthesized proteins and, hence, the polarity of the turning response are determined by mRNA-specific regulation. For class 1 (Ca^{2+}-dependent) guidance cues like netrin-1, Ca^{2+} is a candidate switch mechanism[3], especially because laminin seems to switch netrin-induced attraction to repulsion by lowering cAMP and thereby reducing Ca^{2+}-induced Ca^{2+} release[26,33]. Global translation initiation regulation combined with mRNA-specific regulation is consistent with our finding that enolase protein levels do not change with netrin-1 stimulation, despite both the presence of enolase mRNA and the upregulation of global translation initiation[10]. Further studies will be needed to test this idea, especially the identity of proteins synthesized in attractive versus repulsive conditions.

mRNA-specific regulation may not entail separate RNA-binding proteins. Proteomic and colocalization studies have shown that RNP

complexes consist of multiple RNA-binding proteins and can transport several different mRNAs[43]. Consistent with this, we have shown that Vg1RBP also interacts with cofilin mRNA, which is translated in response to the chemorepellent Slit2 (ref. 8). It may be that in attractive conditions, Vg1RBP activates β-actin translation after being phosphorylated by Src, as occurs for the chick homolog of Vg1RBP, ZBP1 (ref. 20), whereas an alternative signaling pathway causes Vg1RBP to activate cofilin translation but suppress β-actin translation in repulsive conditions. The exact sequence of signaling between DCC and Src remains largely unknown, but Src might in turn be activated by DCC through direct binding or via focal adhesion kinase (FAK), which interacts with DCC[44].

The differential sensitivity to β-actin translation inhibition of attraction versus repulsion and collapse suggests that repulsion and attraction are not simply mirror-symmetrical processes but rather operate through distinct pathways. This may not be surprising because attraction involves near-side filopodial extension, whereas repulsion involves near-side filopodial withdrawal[16]. Indeed, it is thought that repulsive turning is essentially localized collapse, because guidance cues or drugs that cause collapse when added globally generally elicit repulsive turning when presented asymmetrically[45]. Consistent with this, the repellent Slit2 does not induce β-actin synthesis, and indeed results in a significant decrease in β-actin[8], possibly caused by depolymerization due to Slit2-induced cofilin synthesis, combined with suppression of β-actin translation. Similarly, we observed that a gradient of netrin-1 in repulsive conditions did not induce near-side β-actin synthesis, but rather caused a slight, though nonsignificant, decrease of β-actin on the near side. This model predicts that although inhibition of β-actin synthesis does not block repulsive turning, deregulation of β-actin synthesis might. In agreement with this model, an independent study detects a decrease of β-actin on the near side in response to a repulsive gradient and shows that an antisense oligonucleotide directed against the zipcode in the 3′ UTR of β-actin mRNA blocks both the asymmetrical decrease of β-actin and repulsive turning[40].

We have provided here evidence that netrin-1 induces a rapid, local, asymmetric increase in β-actin mRNA translation in retinal growth cones, which is necessary for the attractive turning response and might be achieved via directed transport of Vg1RBP and/or asymmetrical translation initiation. We speculate that newly synthesized β-actin may provide spatially targeted *de novo* nucleation sites for actin polymerization and hence direct the migration of the growth cone toward the cue (**Supplementary Fig. 3** online). Our data agree with those previously obtained in fibroblasts[19] and suggest that similar mechanisms occur to direct migration in the two cell types. Together with the fact that numerous cytoskeletal mRNAs and cytoskeletal-regulatory protein mRNAs have been identified in axons, this suggests that the ability of growth cones to transduce external gradients into matching internal asymmetries of cytoskeletal protein synthesis might be a conserved mechanism.

METHODS

Reagents. Purified netrin-1 (ref. 46) was used at 300 ng ml^{-1} for bath-application, 10 μg ml^{-1} in turning assays and 5 μg ml^{-1} in eIF4E-BP1 assays. CHX (25 μM, Sigma) and rapamycin (10 nM, Calbiochem) were bath-applied to retinal cultures immediately before the addition of netrin-1. Antibodies were as follows: β-actin (1:400, AC15, Abcam), enolase (1:100, H300, Santa Cruz Biotechnologies), Vg1RBP antiserum[47], Ser65-phosphorylated eIF-4EBP1 and total eIF-4EBP1 (1:50 and 1:67, Cell Signaling Technology). Vg1RBP antiserum was affinity purified using recombinant Vg1RBP protein. The Zenon Rabbit IgG Labeling Kit (Molecular Probes) was used for 4EBP double staining (5:1 Zenon reagent/primary antibody ratio for phospho-4EBP, 3:1 for total-4EBP).

Morpholinos and plasmids. AMOs conjugated to lissamine were designed and supplied by GeneTools: *X. laevis* β-actin AMO, 5′-CAATATCGTCTTC CATTGTGATCTG-3′; control, 5′-CCTCTTACCTCAGTTACAATTTATA-3′. pCS2 Kaede–3′ UTR was generated by fusing CoralHue *Kaede* (MBL; accession no. AB085641) to the 3′ UTR of *X. laevis* β-actin (Accession No. BC041203) into pCS2+. The Kaede–Δ3′ UTR construct lacks the first 419 bp of the 3′-UTR. We used pET21d-Vg1RBP-GFP (accession no. AF064634)[48] and pSP64T-Vg1RBP-eGFP as described[49]. See **Supplementary Methods** online for cloning details.

Immunoprecipitation and β-actin mRNA detection. Analysis of Vg1RBP and β-actin mRNA interaction was performed as described[8]. PCR was performed with the following primers: β-actin mRNA, 5′-CCTGTGCAGGAAGATCAC AT-3′ and 5′-TGTTAAAGAGAATGAGCCCC-3′; S1P1 mRNA, 5′-ATCGGC AACTTGGCTCTTTCGG-3′ and 5′-ATTCCCCCTCATCTTTCTGCGG-3′; GAPDH mRNA: 5′-GACTCCACCCACGGCCGC-3′ and 5′-CCATTGAAGTC AGTGGAG-3′.

***In situ* hybridization.** Probes were generated for a 446-bp fragment (1,172–1,618 bp, accession no. BC041203) comprising the 3′ UTR of β-actin mRNA, which was amplified by PCR using primers 5′-AAAGGATCCAAGGACAG ACCCTTTCAACATG-3′ and 5′-AAAGAATTCGTGAAACAACATAAGTTT TATTTTTTC-3′ and cloned into pBluescript. For FISH, retinal cultures from stage 33/34 embryos were fixed in 4% PFA, 7.5% sucrose in PBS for 1 h at RT. Hybridization was performed using 0.6 ng μl^{-1} riboprobes and subsequent detection of β-actin mRNA and Vg1RBP (1:300) was perfomed as described[12,50].

Quantification of fluorescence intensity. Immunostaining, image capture and quantification of fluorescence intensity were carried out as described[8]. Statistical analyses were performed using InStat3 (GraphPad Software).

Growth cone turning and gradient assay. Gradients of diffusible netrin-1 protein and Sema3A supernatant (or control) were established as described[10,30]. In 5-min gradient stimulation experiments, a source of netrin-1 was placed at 90° to the direction of the axon shaft. Images were taken every 30 s for 5 min. Samples were rapidly fixed and analyzed immediately (in case of Vg1RBP-eGFP), stained using β-actin antibodies to detect β-actin protein levels, or double-stained using phospho-4EBP and total-4EBP antibodies to detect 4EBP phosphorylation levels. For the 4EBP experiments, the pipette was placed 67 μm from the growth cone. For asymmetry experiments, the growth cone was bisected into two equal areas by a line drawn through the axon shaft (90° to the pipette) by an experimenter blind to the direction of the gradient. 4EBP phosphorylation on each side of the growth cone was calculated as phospho-4EBP intensity divided by total-4EBP intensity. The center of mass was analyzed using ImageJ software (NIH). The background fluorescence level was subtracted from all pixels of the growth cone. The centers of mass of phospho-4EBP and total-4EBP fluorescence within the growth cone were calculated as the average of all pixel locations weighted by intensity. Filopodium length was measured using Open*lab* software (Improvision). Growth cones showing fewer than two filopodia on each side were excluded from the analysis, as were filopodia shorter than 1 μm.

Live cell imaging. Stage 24 Kaede–β-actin 3′ UTR injected retinal primordia were cultured for 24 h and imaged for 30 min. Kaede-positive growth cones were selected and the whole neurite including the axon shaft was photoconverted by exposure to 340- to 380-nm irradiation. Images were taken every 2.5 min and the intensities of the signals were quantified in each frame and averaged per 5 min. In some cases, axons were severed from their cell bodies before the photoconversion. Fluorescence intensity was normalized to the first frame after photoconversion and presented against relative time (min).

Stage 33/34 Vg1RBP-eGFP–injected retinal primordial cells were cultured for 24 h. Images of Vg1RBP-eGFP positive growth cones viewed at 100× with a Nikon inverted microscope equipped with a cooled CCD camera were captured every 12 s under reduced fluorescence intensities to avoid bleaching. To measure granule speed, images were captured every second. Open*lab* and Volocity software (Improvision) were used to calculate the number and speed of granules.

Note: Supplementary information is available on the Nature Neuroscience website.

ACKNOWLEDGMENTS

We thank M. Spira for suggesting use of Kaede–β-actin 3′ UTR; R. Adams for suggesting use of the Zenon labeling kit; J. Ireland and B. Kvinlaug for preliminary data on β-actin translation; J. Zheng, D. Campbell and L. Strochlic for sharing unpublished data; A. Dwivedy, I. Pradel and K. Zivraj for technical assistance; L. Poggi and J. Falk for help with image analysis; and W. Harris, M. Piper and D. Campbell for comments on the manuscript. This work was supported by a Croucher Scholarship (K.-M.L.), an EMBO Long Term Fellowship (F.P.G.v.H.), an NSF Graduate Research Fellowship (A.C.L.), a BBSRC Studentship (R.A.) and a Wellcome Trust Programme Grant (C.E.H.).

AUTHOR CONTRIBUTIONS

K.-M.L. did the experiments on β-actin synthesis and function in **Figures 3**, **6**, **7** and **Supplementary Figure 2**. F.P.G.v.H. did the experiments on Vg1RBP in **Figures 1**, **2**, **4**, **Supplementary Figures 1** and **2k–o** and **Supplementary Videos 1–4**. A.C.L. did the gradient assays on 4EBP and β-actin in **Figures 5** and **6e**. R.A. and N.S. provided Vg1RBP reagents and constructs and discussed experiments. K.-M.L., F.P.G.v.H., A.C.L. and C.E.H. wrote the manuscript and discussed experiments.

COMPETING INTERESTS STATEMENT

The authors declare that they have no competing financial interests.

Published online at http://www.nature.com/natureneuroscience
Reprints and permissions information is available online at http://npg.nature.com/reprintsandpermissions/

1. Henley, J. & Poo, M.M. Guiding neuronal growth cones using Ca^{2+} signals. *Trends Cell Biol.* **14**, 320–330 (2004).
2. Guirland, C., Suzuki, S., Kojima, M., Lu, B. & Zheng, J.Q. Lipid rafts mediate chemotropic guidance of nerve growth cones. *Neuron* **42**, 51–62 (2004).
3. Wen, Z., Guirland, C., Ming, G.L. & Zheng, J.Q.A. CaMKII/calcineurin switch controls the direction of Ca^{2+}-dependent growth cone guidance. *Neuron* **43**, 835–846 (2004).
4. Zheng, J.Q. Turning of nerve growth cones induced by localized increases in intracellular calcium ions. *Nature* **403**, 89–93 (2000).
5. Li, Y. *et al.* Essential role of TRPC channels in the guidance of nerve growth cones by brain-derived neurotrophic factor. *Nature* **434**, 894–898 (2005).
6. Lohof, A.M., Quillan, M., Dan, Y. & Poo, M.M. Asymmetric modulation of cytosolic cAMP activity induces growth cone turning. *J. Neurosci.* **12**, 1253–1261 (1992).
7. Ming, G.L. *et al.* Adaptation in the chemotactic guidance of nerve growth cones. *Nature* **417**, 411–418 (2002).
8. Piper, M. *et al.* Signaling mechanisms underlying slit2-induced collapse of *Xenopus* retinal growth cones. *Neuron* **49**, 215–228 (2006).
9. Wu, K.Y. *et al.* Local translation of RhoA regulates growth cone collapse. *Nature* **436**, 1020–1024 (2005).
10. Campbell, D.S. & Holt, C.E. Chemotropic responses of retinal growth cones mediated by rapid local protein synthesis and degradation. *Neuron* **32**, 1013–1026 (2001).
11. Shestakova, E.A., Singer, R.H. & Condeelis, J. The physiological significance of β-actin mRNA localization in determining cell polarity and directional motility. *Proc. Natl. Acad. Sci. USA* **98**, 7045–7050 (2001).
12. Bassell, G.J. *et al.* Sorting of β-actin mRNA and protein to neurites and growth cones in culture. *J. Neurosci.* **18**, 251–265 (1998).
13. Willis, D. *et al.* Differential transport and local translation of cytoskeletal, injury-response, and neurodegeneration protein mRNAs in axons. *J. Neurosci.* **25**, 778–791 (2005).
14. Zhang, H.L. *et al.* Neurotrophin-induced transport of a β-actin mRNP complex increases β-actin levels and stimulates growth cone motility. *Neuron* **31**, 261–275 (2001).
15. Zhang, H.L., Singer, R.H. & Bassell, G.J. Neurotrophin regulation of β-actin mRNA and protein localization within growth cones. *J. Cell Biol.* **147**, 59–70 (1999).
16. Yuan, X.B. *et al.* Signalling and crosstalk of Rho GTPases in mediating axon guidance. *Nat. Cell Biol.* **5**, 38–45 (2003).
17. Gebauer, F. & Hentze, M.W. Molecular mechanisms of translational control. *Nat. Rev. Mol. Cell Biol.* **5**, 827–835 (2004).
18. Kloc, M., Zearfoss, N.R. & Etkin, L.D. Mechanisms of subcellular mRNA localization. *Cell* **108**, 533–544 (2002).
19. Condeelis, J. & Singer, R.H. How and why does β-actin mRNA target? *Biol. Cell* **97**, 97–110 (2005).
20. Huttelmaier, S. *et al.* Spatial regulation of β-actin translation by Src-dependent phosphorylation of ZBP1. *Nature* **438**, 512–515 (2005).
21. Yisraeli, J.K. VICKZ proteins: a multi-talented family of regulatory RNA-binding proteins. *Biol. Cell.* **97**, 87–96 (2005).
22. Sundell, C.L. & Singer, R.H. Requirement of microfilaments in sorting of actin messenger RNA. *Science* **253**, 1275–1277 (1991).
23. Lopez de Heredia, M. & Jansen, R.P. mRNA localization and the cytoskeleton. *Curr. Opin. Cell Biol.* **16**, 80–85 (2004).
24. Deiner, M.S. *et al.* Netrin-1 and DCC mediate axon guidance locally at the optic disc: loss of function leads to optic nerve hypoplasia. *Neuron* **19**, 575–589 (1997).
25. Campbell, D.S. *et al.* Semaphorin 3A elicits stage-dependent collapse, turning, and branching in *Xenopus* retinal growth cones. *J. Neurosci.* **21**, 8538–8547 (2001).
26. Hopker, V.H., Shewan, D., Tessier-Lavigne, M., Poo, M. & Holt, C. Growth-cone attraction to netrin-1 is converted to repulsion by laminin-1. *Nature* **401**, 69–73 (1999).
27. Takei, N., Kawamura, M., Hara, K., Yonezawa, K. & Nawa, H. Brain-derived neurotrophic factor enhances neuronal translation by activating multiple initiation processes: comparison with the effects of insulin. *J. Biol. Chem.* **276**, 42818–42825 (2001).
28. Wilkie, G.S., Dickson, K.S. & Gray, N.K. Regulation of mRNA translation by 5′- and 3′-UTR-binding factors. *Trends Biochem. Sci.* **28**, 182–188 (2003).
29. Ando, R., Hama, H., Yamamoto-Hino, M., Mizuno, H. & Miyawaki, A. An optical marker based on the UV-induced green-to-red photoconversion of a fluorescent protein. *Proc. Natl. Acad. Sci. USA* **99**, 12651–12656 (2002).
30. de la Torre, J.R. *et al.* Turning of retinal growth cones in a netrin-1 gradient mediated by the netrin receptor DCC. *Neuron* **19**, 1211–1224 (1997).
31. Gingras, A.C. *et al.* Hierarchical phosphorylation of the translation inhibitor 4E–BP1. *Genes Dev.* **15**, 2852–2864 (2001).
32. Eng, H., Lund, K. & Campenot, R.B. Synthesis of beta-tubulin, actin, and other proteins in axons of sympathetic neurons in compartmented cultures. *J. Neurosci.* **19**, 1–9 (1999).
33. Ooashi, N., Futatsugi, A., Yoshihara, F., Mikoshiba, K. & Kamiguchi, H. Cell adhesion molecules regulate Ca^{2+}-mediated steering of growth cones via cyclic AMP and ryanodine receptor type 3. *J. Cell Biol.* **170**, 1159–1167 (2005).
34. Kuhn, T.B., Brown, M.D., Wilcox, C.L., Raper, J.A. & Bamburg, J.R. Myelin and collapsin-1 induce motor neuron growth cone collapse through different pathways: inhibition of collapse by opposing mutants of rac1. *J. Neurosci.* **19**, 1965–1975 (1999).
35. Hansen, W.J., Cowan, N.J. & Welch, W.J. Prefoldin-nascent chain complexes in the folding of cytoskeletal proteins. *J. Cell Biol.* **145**, 265–277 (1999).
36. Wang, J. *et al.* Reversible glutathionylation regulates actin polymerization in A431 cells. *J. Biol. Chem.* **276**, 47763–47766 (2001).
37. Kislauskis, E.H., Zhu, X. & Singer, R.H. β-actin messenger RNA localization and protein synthesis augment cell motility. *J. Cell Biol.* **136**, 1263–1270 (1997).
38. Lewis, A.K. & Bridgman, P.C. Nerve growth cone lamellipodia contain two populations of actin filaments that differ in organization and polarity. *J. Cell Biol.* **119**, 1219–1243 (1992).
39. Oleynikov, Y. & Singer, R.H. Real-time visualization of ZBP1 association with β-actin mRNA during transcription and localization. *Curr. Biol.* **13**, 199–207 (2003).
40. Yao, J., Sasaki, Y., Wen, Z., Bassell, G.J. & Zheng, J.Q. An essential role for β-actin mRNA localization and translation in Ca^{2+}-dependent growth cone guidance. *Nat. Neurosci.* **9**, 1265–1273 (2006).
41. Rousseau, D., Kaspar, R., Rosenwald, I., Gehrke, L. & Sonenberg, N. Translation initiation of ornithine decarboxylase and nucleocytoplasmic transport of cyclin D1 mRNA are increased in cells overexpressing eukaryotic initiation factor 4E. *Proc. Natl. Acad. Sci. USA* **93**, 1065–1070 (1996).
42. Brunet, I. *et al.* The transcription factor Engrailed-2 guides retinal axons. *Nature* **438**, 94–98 (2005).
43. Kanai, Y., Dohmae, N. & Hirokawa, N. Kinesin transports RNA: isolation and characterization of an RNA-transporting granule. *Neuron* **43**, 513–525 (2004).
44. Liu, G. *et al.* Netrin requires focal adhesion kinase and Src family kinases for axon outgrowth and attraction. *Nat. Neurosci.* **7**, 1222–1232 (2004).
45. Fan, J. & Raper, J.A. Localized collapsing cues can steer growth cones without inducing their full collapse. *Neuron* **14**, 263–274 (1995).
46. Shirasaki, R., Mirzayan, C., Tessier-Lavigne, M. & Murakami, F. Guidance of circumferentially growing axons by netrin-dependent and -independent floor plate chemotropism in the vertebrate brain. *Neuron* **17**, 1079–1088 (1996).
47. Zhang, Q. *et al.* Vg1 RBP intracellular distribution and evolutionarily conserved expression at multiple stages during development. *Mech. Dev.* **88**, 101–106 (1999).
48. Yaniv, K., Fainsod, A., Kalcheim, C. & Yisraeli, J.K. The RNA-binding protein Vg1 RBP is required for cell migration during early neural development. *Development* **130**, 5649–5661 (2003).
49. Chang, P. *et al.* Localization of RNAs to the mitochondrial cloud in *Xenopus* oocytes through entrapment and association with endoplasmic reticulum. *Mol. Biol. Cell* **15**, 4669–4681 (2004).
50. Blichenberg, A. *et al.* Identification of a *cis*-acting dendritic targeting element in MAP2 mRNAs. *J. Neurosci.* **19**, 8818–8829 (1999).